Proceedings of the ASME 2010 3rd Joint US-European Fluids Engineering Summer Meeting and 8th International Conference on Nanochannels, Microchannels, and Minichannels
FEDSM-ICNMM2010
August 1-5, 2010, Montreal, Canada

FEDSM-ICNMM2010-30592

DEVELOPMENT OF STENT STRUT PATTERN FOR CEREBRAL ANEURYSM

Toshio NAKAYAMA
Biomedical Engineering, Tohoku University
Sendai, Miyagi, Japan

Shinkyu JEONG
Institute of Fluid Science, Tohoku University
Sendai, Miyagi, Japan

Srinivas KARKENAHALLI
Department of Aeronautical Engineering
Sydney, NSW, Australia

Makoto OHTA
Institute of Fluid Science, Tohoku University
Sendai, Miyagi, Japan

ABSTRACT

Background and purpose: Stent implantation (stenting) in intracranial arteries is termed as endovascular treatment. The number of such cases has been increasing worldwide because the surgical damage resulting from stenting seem to be less than that of other treatments. The role of stenting for cerebral aneurysms is to reduce the blood flow speed in cerebral aneurysms. We have developed a computational fluid dynamics (CFD) system using a realistic stent and blood vessel and have studied the effect of the stent. Results of our study showed the stent strut pattern and stenting position to be very effective for reducing the blood flow speed in cerebral aneurysms. We have in describe the designing method used to design the stent strut pattern which reduces both the blood flow speed and the wall shear stress (WSS).

Methods: An idealized aneurysm, a parent artery, and various stent shapes were used. The shape of the parent artery was a straight pipe and the aneurysm was a sphere. The stent was implanted in the neck of the aneurysm. The porosity remained of 80%, and the width of the stent strut ranged from 90 to 160[μm]. The stent strut height was fixed at a constant 150 [μm]. For the constructed shape data, a tetrahedron numerical mesh was generated. Calculation using the finite volume method was performed by a commercial solver. The optimization method was applied to the CFD results, and the stent strut patterns that reduced the blood flow speed and the WSS most were determined.

Conclusion: The development method of stent strut pattern was proposed. Various stent strut patterns to reduce blood flow speed and WSS in/on cerebral aneurysm were tested. The stent strut pattern that reduced the blood flow speed and that reduced the WSS were determined. In the future works, the number of CFD cases should be increased and the optimal stent strut pattern determined.

INTRODUCTION

The rupture of a cerebral aneurysm causes massive bleeding in the brain which is life-threatening and has a high probability of brain sequelae. Brain attack or stroke is the third leading cause of death [1] and cannot be ignored. Treatment of unruptured cerebral aneurysms is very useful. There are surgical treatment and endovascular treatment in unruputure cerebral aneurysm. As endovascular treatment is minimally invasive, puts little burden on the patient and facilitates rehabilitation, the endovascular therapies have the focus of attention.

Recently, endovascular therapies utilizing coil embolization or stent implantation have been utilized as minimally invasive treatments. The effects of stenting of cerebral arterial aneurysms on internal blood flow reduction have been investigated by numerical [2-6] and experimental [7-9] flow studies. Aenis et al. performed numerical studies with a stent strut aligned perpendicular on the aneurysm neck, the results of which suggested that the flow speed in an aneurysm decreased after stent implantation using numeric studies [2]. Ohta et al. carried out a numerical analysis with two stent struts aligned perpendicular or parallel to the parent artery on the aneurysm neck, and showed that the flow pattern in the aneurysm neck was changed, even though the porosity stayed the same [3]. They also used two-dimensional models with a parent artery, a smaller branching artery, and an aneurysm located at the bifurcation, before and after stent placement, for simulation of rheological changes and found that the viscosity of blood increased after stenting [4]. Hirabayashi et al.

Copyright © 2010 by ASME

investigated the effect of stent positioning on velocity reduction in an ideal aneurysm using the lattice Boltzmann method [5]. In these cited numerical studies, stent shapes were modeled by computer aided design (CAD) and only the shapes of blood vessels were reconstructed from medical images. The blood flow in a cerebral arterial aneurysm is related to the stenting position [8]. Nakayama et al. developed the computationa fluid dynamics (CFD) system using a realistic stent and cerebral aneurysm [9]. Their results indicate that the stent strut pattern and stenting position are very effective in reducing the blood flow speed I and wall shear stress (WSS) cerebral aneurysms. Srinivas et al. developed the optimization of stent strut position [10]. But this research study was two-dimensional.

Therefore, in the present report, we describe the design of three-dimensional optimization method of stent strut pattern which reduces both the blood flow speed and WSS.

MATERIALS AND METHODS

3-D Reconstruction of Cerebral Aneurysm

For the purposes of simplification, an idealized shape was used for this calculation. The parent blood vessel was a straight pipe and the aneurysm was a sphere. A straight pipe was used for the connection between the parent blood vessel and the aneurysm to make a circular shape at the neck of aneurysm. The diameter of the parent blood vessel was 4 [mm], its length was 50 [mm], and the diameter of the aneurysm was 8[mm]. For construction of the blood vessel and aneurysm Rapid Prototyping software (MagicsRP12.1 (Materialise, Belgium)) was used. Figure 1 shows the shape of the constructed blood vessel and that of the aneurysm.

3-D Reconstruction of Intracranial Stent

An idealized stent shape was used. Figure 2 shows the stent strut pattern. The stent strut was arranged at the center of the aneurysm neck. The stent was implanted at a position 1.9 [mm] from the center of the blood vessel. For purposes of simplification, the stent strut was implanted only in the cerebral aneurysm neck, not in other blood vessel wall parts.

In all cases, porosity was maintained at 80%, and the width and length of the stent strut was changed, CFD being performed in each of the cases. From the results, the

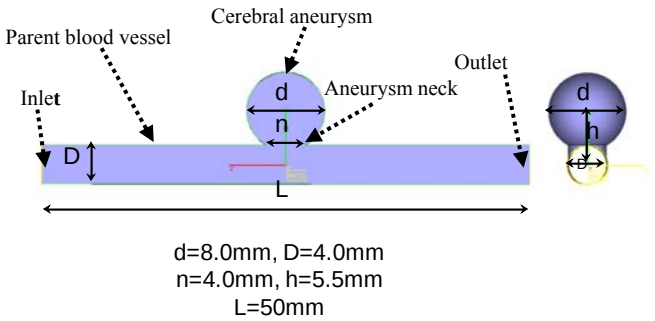

Figure 1 The blood vessel shape

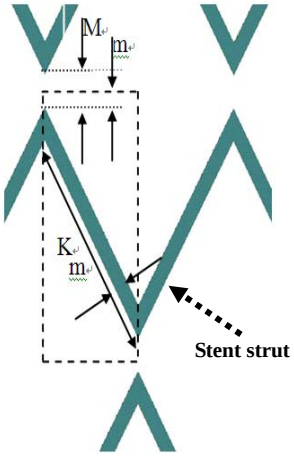

Figure 2 The basic stent strut pattern

combination of the lowest blood flow speed and lowest WSS was considered to be the best stent strut pattern.

In the part enclosed by dotted line, the area of the stent strut was maintained at 20% by adjusting the stent strut length and width. As a result, the porosity of this stent remained at 80% in this area, i.e., the porosity of one strut, not the porosity of the aneurysm neck area.

The width of the commercial stent strut is about 100[μm]. The stent strut width was assumed to be from 90 to 160[μm] and, the stent strut height was assumed to be constant of 150 [μm]. Seven stent strut width were examined: 95[μm], 105[μm], 115[μm], 125[μm], 135[μm], 145[μm], and 155[μm], and CFD analysis was performed for these seven cases and for the case of no stent. From the results, the stent strut pattern resulting in the biggest decrease was identified. Figure 3 shows the stent strut pattern on the aneurysm neck.

Numerical Simulation

The constructed shape data were transferred to a supercomputer (Silicone Graphics Prism, SGI Japan, Ltd, Japan) and a tetrahedron numerical mesh was generated with tetrahedron using a commercial software package (Gambit 2.2.30, Fluent Inc., NH). The number of mesh was from 500,000 to 800,000 in all cases. Figure 4 shows fine mesh near the stent strut. By Size function was used near the stent strut, the size of mesh near the stent strut was finer than that of the other parts.

The blood flow was simplified as an isothermal, incompressible, laminar Newtonian flow with a density of 1050 [kg/m3] and a viscosity of 0.0035 [Pa s].

The boundary conditions of the inlet, outlet, vessel, aneurysm wall, and stent are time-independent. A flat flow velocity profile of 0.200[m/s] was introduced on the inlet to be consistent with the Reynolds Number of 240. A constant pressure was set on the outlet. No-slip condition was employed on the vessel, aneurysm, and stent.

Copyright © 2010 by ASME

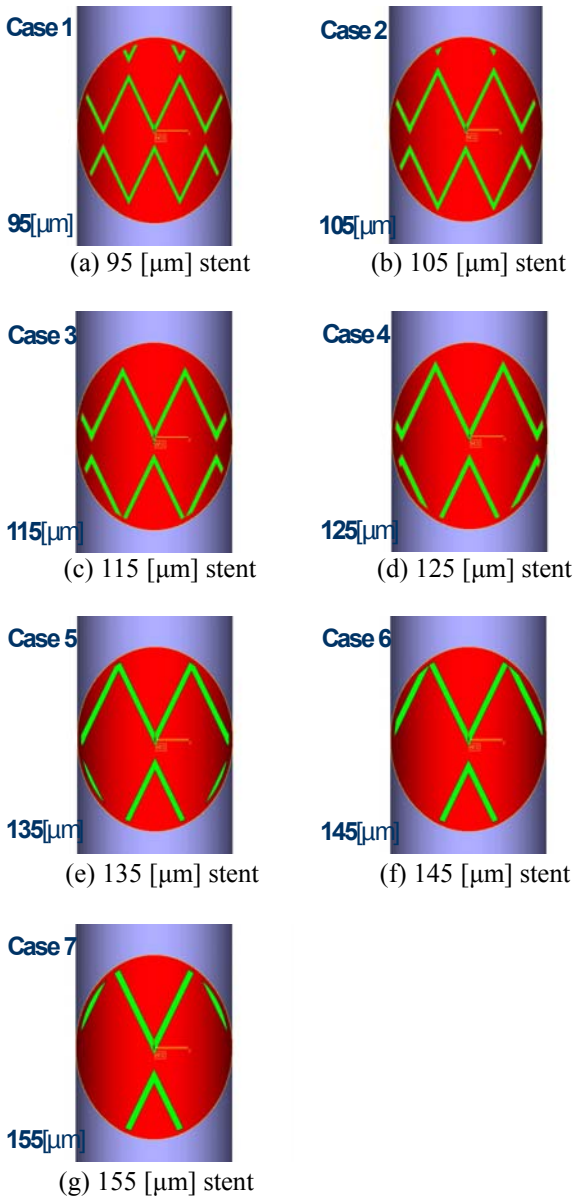

(a) 95 [μm] stent (b) 105 [μm] stent

(c) 115 [μm] stent (d) 125 [μm] stent

(e) 135 [μm] stent (f) 145 [μm] stent

(g) 155 [μm] stent

Figure 3 The stent strut pattern on the neck of aneurysm

The basic equations of continuity and the Navier-Stokes equation were solved to determine the flow field. The calculation using the finite volume method was performed by a commercial solver (Fluent 6.2.16, Fluent Inc. NH). The computer (Prism, SGI Corporation) was used for the calculation.

Optimization

In the spirit of the method used, namely, exploration of design space, one examines a large number of candidate designs and evolves an optimum. The results of CFD analysis were evaluation for the each objective functions. The each objective functions were the maximum velocity and WSS. This

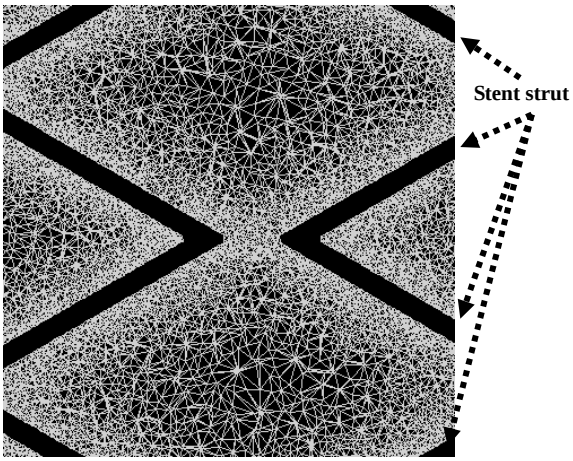

Figure 4 The fine mesh near the stent strut

evaluation method was followed by the process of Multi-Objective Genetic Algorithm and Kriging [11], to produce a response surface [12], which represents the relationship between the objective functions and the design variables. The process essentially predicts unknown values from the data collected by computations. The procedure also yields what are called nondominated solutions. These contain several optimized solutions, allowing the designer to select the one that suits a given situation. In this paper, an in-house software was used for optimization.

RESULTS

From the CFD results, Figure 5 shows the maximum and mean blood flow speed in the cerebral aneurysm, and Figure 6 shows the maximum and mean WSS on the cerebral aneurysm. The maximum blood flow speed in the cerebral aneurysm was decreased the most when a 125 [μm] stent was implanted. The maximum blood flow speed has increased though the width of the stent strut increased or decreased. The mean blood flow speed showed a different tendency. It decreased most in the case of 95 [μm] implanted stent and decreased least in the case of the 145 [μm] implanted stent. The mean blood flow speed tended to increase with increasing width of stent strut. The 95 [μm] stent was the worst case of maximum blood flow speed and the best case of mean blood flow speed. The maximum WSS was decreased most when 105 [μm] stent was implanted and the mean WSS was decreased most when 95 [μm] stent was implanted. The maximum WSS was the least decreased when 155 [μm] stent was implanted and the mean WSS was the most decreased case when 155 [μm] stent was implanted. The tendency of mean WSS increased with increasing stent strut width but the tendency of maximum WSS was not apparent. The blood flow speed and WSS in all cases of stent implantation were lower than in the case of no-Stent.

Figure 7 shows the position of the cut plane. Plane A is the center of the aneurysm. Plane B is 1/3 of the aneurysm neck. Plane C is the cross section of the aneurysm neck.

Copyright © 2010 by ASME

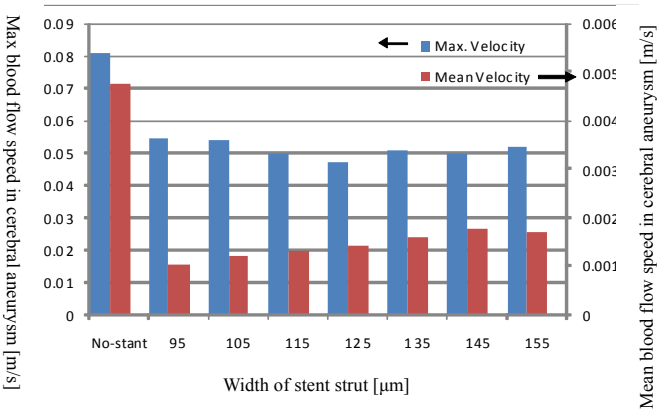

Figure 5 The maximum & the mean blood flow speed in cerebral aneurysm

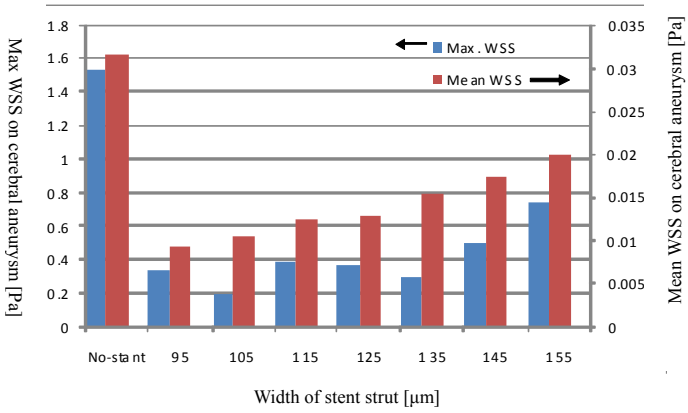

Figure 6 The maximum & the mean WSS on cerebral aneurysm

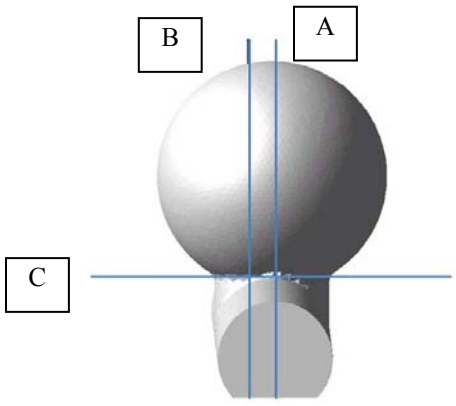

Figure7 Cut Plane

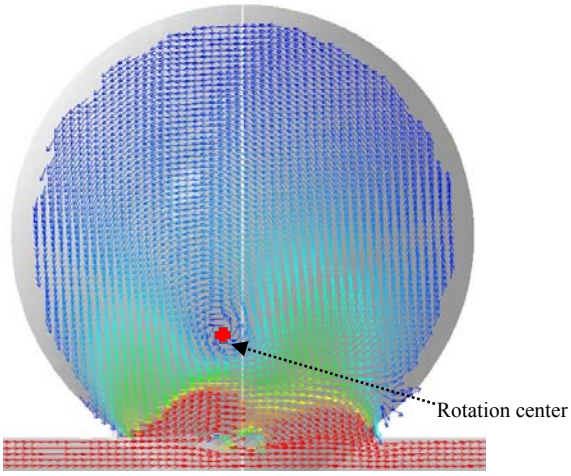

(a) Plane A

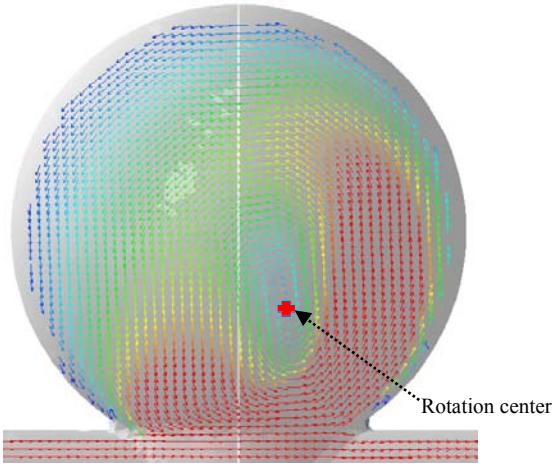

(b) Plane B

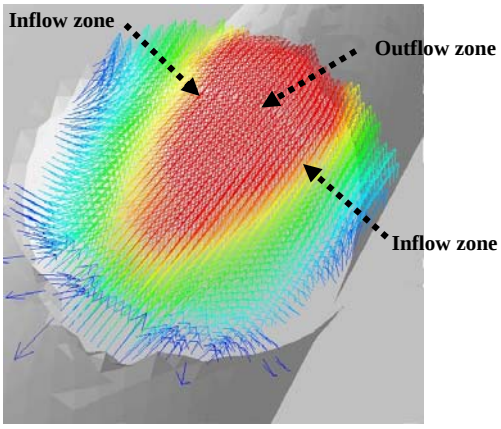

(c) Plane C

Figure 8 Velocity vector (no-stent)

Copyright © 2010 by ASME

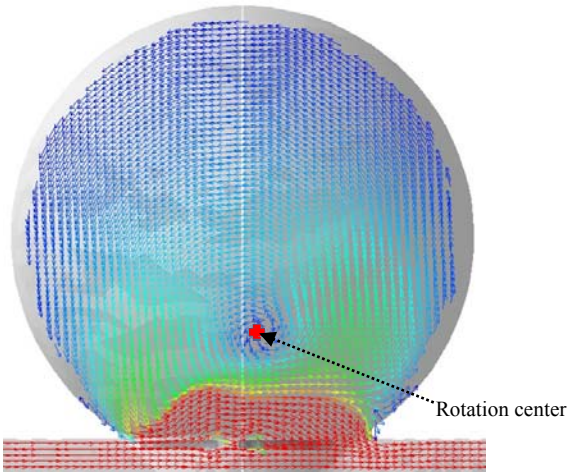

(a) Plane A

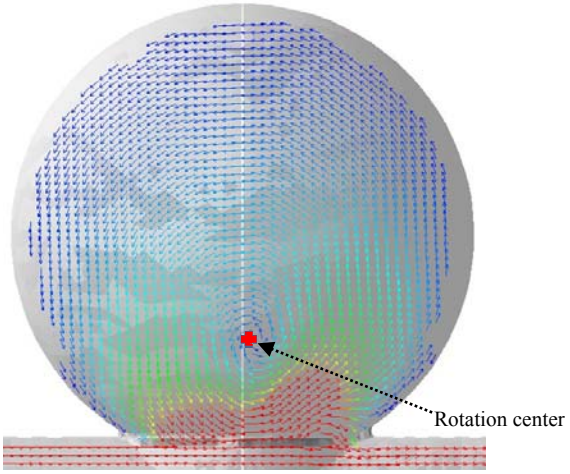

(b) Plane B

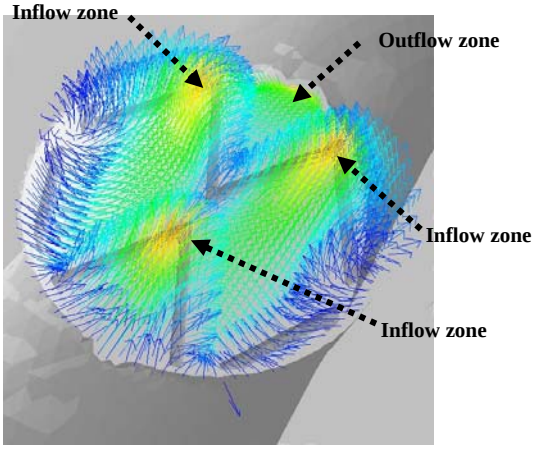

(c) Plane C

Figure 9 Velocity vector (125 [μm])

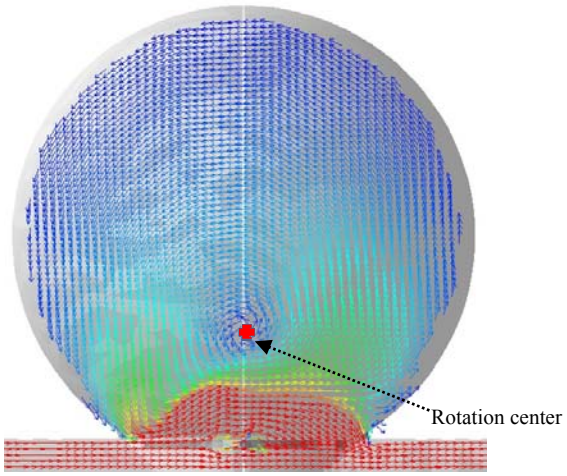

(a) Plane A

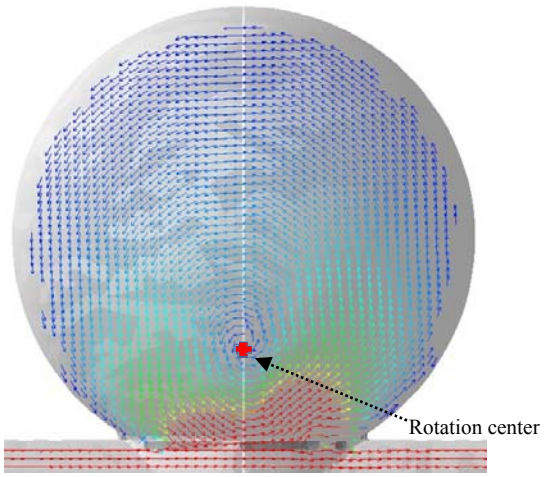

(b) Plane B

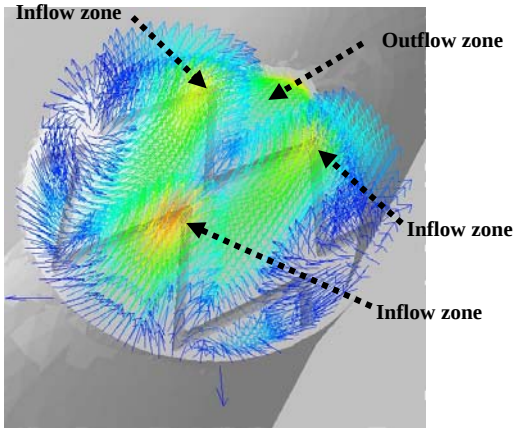

(c) Plane C

Figure 10 Velocity vector (105 [μm])

Copyright © 2010 by ASME

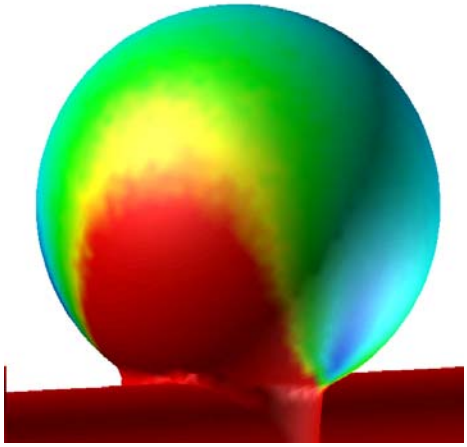

(a) no-stent case

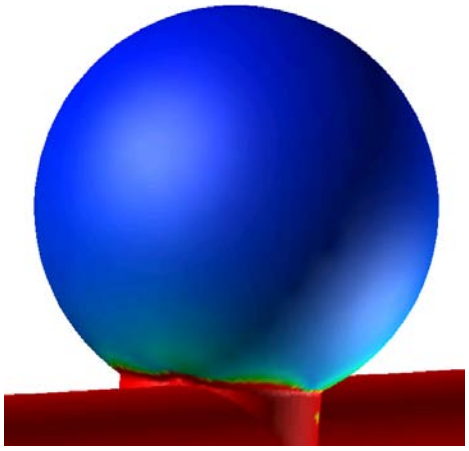

(b) 105 [μm]

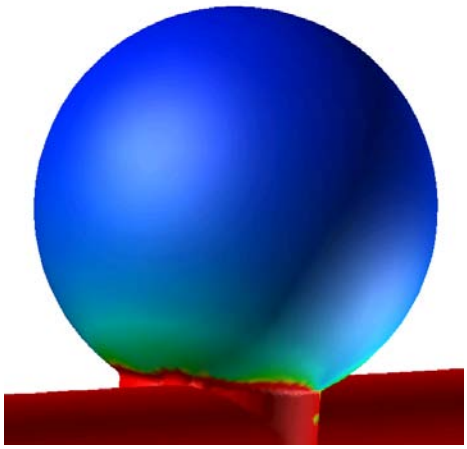

(c) 125 [μm]

Figure 11 Wall Shear Stress contour

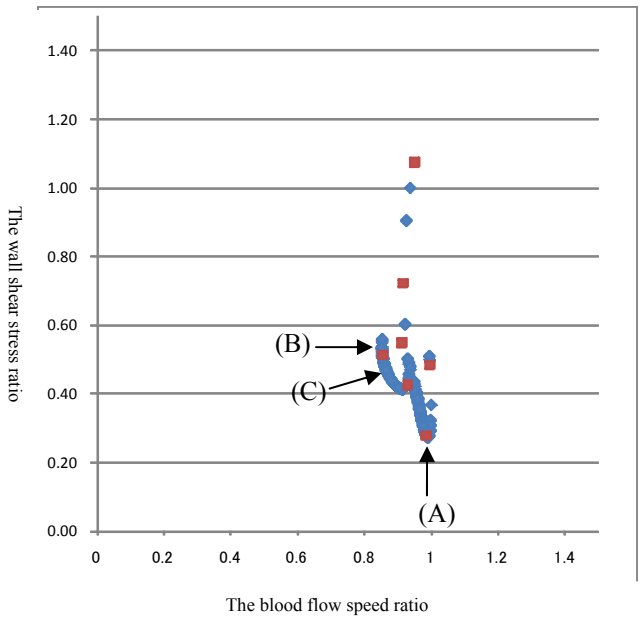

Figure 12 Non-dominated front for stent strut pattern (Blue) and CFD results (Red)

Figure 8 shows the velocity vector in the case of no stent. The colors indicate the blood flow speed and the arrows indicate of the blood flow. The center of the distal position in the aneurysm neck is the blood flow outflow zone of the aneurysm. The side of distal in aneurysm neck is a blood flow inflow zone of aneurysm. From Figure 8(b), a high-speed area reaches more than half of the aneurysm. Figure 9 shows the velocity vector when the 125 [μm] stent was implanted. The colors indicate the blood flow speed and the arrow indicate the direction of blood flow. This is the most reduced maximum blood flow case. The center of the proximal stent strut and the edge of distal stent strut area is inflow zone to aneurysm. Figure 10 shows the velocity vector when the 105 [μm] stent was implanted. The colors indicate the blood flow speed and the arrow indicate the direction of the blood flow. This is the most reduced maximum WSS case. The inflow zone of the aneurysm is almost same as that in the case of the125 [μm] stent.

The apparent differences are the center of the rotational flow and the velocity distribution on the aneurysm neck. The center of rotational flow in the 105 [μm] stent is more distal than in the 125 [μm] stent. The blood flow speed in the vicinity of the aneurysm wall is reduced, and the WSS on the aneurysm is reduced. The blood flow speed in the proximal position of the 105 [μm] stent case is faster than in the 125 [μm] stent case, the blood flow speed in distal stent strut of 105 [μm] is slower than 125 [μm] case. The blood flow speed in the aneurysm increase.

Figure 11 shows the wall shear stress contour. The colors indicate the wall shear stress value. Figure 11 (a) is the no-stent case, Figure 11 (b) is the 105 [μm] stent strut case, and Figure

Copyright © 2010 by ASME

11 (c) is the 125 [μm] stent strut case. In Figure 11 (a), the high WSS area reaches more than half of the aneurysm. In the cases of stent implantation, there is a high WSS area only in the neighborhood of the distal aneurysm neck. The distribution of WSS on the aneurysm in 105 [μm] stent case is lower than 125[μm] stent case. This WSS distribution is the almost same to 125 [μm].

In Figure 12, the axis is set on two objective functions. The X-axis shows the blood flow speed ratio (each blood flow speed / maximum blood flow speed), and the Y-axis shows the wall shear stress ratio (each wall shear stress / maximum wall shear stress). The results of CFD and the non-dominated points are plotted. We can identify three non-dominated designs, A, B, and C, from Figure 12, which are the minimum blood flow speed case, the minimum WSS case, and the compromise case, respectively. The maximum WSS was the most reduced case (A) when the 103.604 [μm] stent was implanted. The maximum WSS was the least reduced case (B) when the 123.758 [μm] stent was implanted. The compromise case was when the stent 128.167 [μm] was implanted.

DISCUSSION

In this paper, we introduced and tried the optimization method to produce 3D stent strut pattern design. Stent strut patterns that reduce blood flow speed and WSS were obtained from the optimization method.

Optimization

The stent strut position of the implanted stent cannot be determined in a cerebral aneurysm during the operation of endovascular treatment, thus necessitating a stent strut pattern having high performance for cerebral aneurysm treatment. We speculated that a stent strut pattern which had such a high performance could be developed by use of optimization method.

When porosity of 80% was maintained, the length of the stent was generated in relation to width. The beginning point of the stent strut fixed at the center of aneurysm neck. Then, the number of CFD decreased. The design parameter, objective function, and the number of CFD are related. Decreasing the design parameter led to a decrease of the number of CFD in optimization. By decreasing of the number of CFD, it was possible to decrease the stent design time.

In the arrangement of 7 cases, the beginning point of the stent strut was at the center of the aneurysm neck, and was not changed. The effect of the stent implantation point was not considered. For optimization of the stent srtut pattern, it is necessary to search for the blood flow pattern when the beginning point of the stent is changed.

The process of Kriging to produce a response surface which represents the relationship between the objective functions and the design variables was used. Kriging predicts unknown optimum values from the data collected by experiments. First, the number of calculated objective function is 7 cases. This number is not good for optimization. Second, the width of the stent strut was selected as the design parameter, the maximum blood flow speed and the maximum WSS were selected as the objective function. The increase of the design parameter is necessary, and the increase of the objective function is necessary. In the next step, the number of design parameters and objective functions will be increased. But the increase of design parameter influences the number of CFD. To decrease the number of the design parameter Latin hypercube sampling will be carried out.

Accuracy of calculation

In this simulation, the size of the simulated objects are greatly different in scale because the blood vessel is at millimeter scale and the stent strut is at micrometer scale. Therefore, the mesh size was small near the stent strut and gradually enlarged with distance from stent strut. The stent strut divides the blood flow; therefore, a tetrahedron mesh with a high space filling rate was selected. For a low Reynolds number such as that for the blood flow in a cerebral aneurysm, the calculation accuracy of a tetrahedron mesh was lower than that of a hexahedron mesh, and improvement of calculation accuracy will be necessary in the future.

Simulation was performed for all cases. The number of mesh elements of these cases was about from 600,000 to 800,000. Although the arrangement of the tetrahedron mesh in these samples was not the same, the influence on simulation results by the difference of mesh number and arrangement of the tetrahedron mesh is thought to be small.

Stent strut pattern and blood flow pattern

Results of this study show that there is an important relation between stent strut pattern and blood flow.

By stent implantation, the blood flow speed and WSS were reduced. This is because the stent implantation disturbs the blood flow that enters the cerebral aneurysm, i.e., the stent strut changes the direction of blood flow around the neck of the aneurysm.

In Figures 8(b), 9(b), and 10(b), the case of no stent is compared with the case of stent implantation, the blood flow speed in the cerebral aneurysms was reduced as result of the blind effect of stent strut.

In Figure 8(c), 9(c), and 10(c), the case of no stent is compared with the case of stent implantation, It can be seen that the number of inflow zones has increased, and the inflow zone of the distal portion moves in proximally only a little. As the inflow zone of the center proximal stent is generated, the amount of blood flow that enters from the distal side decreases the blood flow speed near the aneurysm wall and WSS is reduced.

CONCLUTION

The development of a stent strut pattern to reduce blood flow speed and WSS in/on cerebral aneurysms was proposed. By design optimization the stent strut patterns that most greatly reduced the blood flow speed, and the WSS were determined.

Copyright © 2010 by ASME

In future works, the number of CFD cases will be increased and we will strive to determine the best stent strut pattern.

ACKNOWLEDGMENTS

This research was partially supported by the Ministry of Education, Science, Sports and Culture, Grant-in-Aid for Young Scientists (B), 21760108, 2008. This research was supported by Core to core project 2008, JSPS. CFD analysis was performed by the super-computer of Institute Fluid Science, Tohoku University.

REFERENCES

1. http://www2.health.ne.jp/images/LVL3/0200002/graph01.gif
2. Aenis, M., Stancampiano, A. P., Wakhloo, A. K. and Lieber, B. B. Modeling of flow in a straight stented and nonstented side wall aneurysm model. J Biomech Eng. 1997, 119, 206-212
3. Ohta M, Hirabayashi M, Wetzel S, Lylyk P, Iwata H, Tsutsumi S, Rüfenacht DA. Impact of Stent Design on Intra-Aneurysmal Flow: A computer simulation study. Interventional Neuroradiology, 2004, 10(Supp2),85-94
4. Ohta M, Wetzel SG, Dantan P, Bachalat C, Lovblad KO, Yilmaz H, Flaud P, Rüfenacht DA. Rheological changes after stenting of a cerebral aneurysm: a finite element modeling approach.Cardiovascular interventional radiology, 2005, 28(6), 768-772,.
5. Hirabayashi M, Ohta M, Barath K., Rufenacht DA., Chopard B. Numerical analysis of the flow pattern in stented aneurysms and its relation to velocity reduction and stent efficiency. Mathematics and Computers in Simulation, 2006, 72, 128-133.
6. Stuhne GR, Steinman DA, Mesh Resolution Requirements for the Numerical Simulation of Flow Through Stented Aneurysms, 2003, Summer Bioengineering Conference
7. Rhee K, Han MH, Cha SH. Changes of flow characteristics by stenting in aneurysm models: influence of aneurysm geometry and stent porosity. Ann. Biomed. Eng., 2002 vol. 30, 894-904.
8. Baráth, Krisztina, Cassot, Francis, Fasel, Jean H.D., Ohta M, Rüfenacht DA. Influence of stent properties on the alteration of cerebral intra-aneurysmal haemodynamics: flow quantification in elastic sidewall aneurysm models. Neurological Research, 2005, 27, Vol. 1,120-128
9. Nakayama T., Ohta M, Rüfenacht DA., Takahashi A. Numerical Simulation of Hemodynamics in Cerebral Arterial Aneurysm using Realistic Stent Data. C Proceedings of the 6th International Symposium on Advanced Fluid Information. 2006 , pp 47-48.
10. Srinivas K., Nakayama T., Ohta M., Obayashi S., Yamaguchi T. Studies on Design Optimization of Coronary Stents, Journal of Medical Devices, 2008, 2, 011004-1-011004-7
11. Donald, R. J., Matthias, S., and William, J. W. Efficient Global Optimization of Expensive Black-Box Function, J. Global Optim., 1998, 13,455-492.
12. Myers, R. H., and Montgomery, D. C., 1995, Response Surface Methodology: Process and Product Optimization Using Designed Experiments, Wiley, New York, pp. 1-8

Copyright © 2010 by ASME